



CM-P00060415

Ref.TH.1664-CERN

PARTICLE PRODUCTION AT LARGE TRANSVERSE MOMENTUM

E.L. Berger <sup>\*)</sup> and D. Branson <sup>+)</sup>  
CERN - Geneva

ABSTRACT

From a simple fragmentation approach to inelastic production at large fixed angles, we obtain an inclusive cross-section which falls as an inverse power of large transverse momentum  $p_T$  and which scales according to  $(p_T/\sqrt{s})$ , both consistent with ISR data. Predictions for charge ratios and associated multiplicities are also presented and compared with available data.

---

\*) On leave from Argonne National Laboratory.

+) On leave of absence from University of Essex, Colchester, England.

Much attention has recently been focused on the observation at the CERN ISR of an unexpectedly large inclusive hadronic cross-section at large transverse momentum  $[1 < p_T < 10(\text{GeV}/c)]^{1)-3)$ , which (for certain  $p_T$ ) grows with energy  $^2)$  through the ISR range, and which shows a preponderance of positively charged hadrons  $^3)$   $[n_+/n_- = 1.33 \pm 0.13$  at  $p_T = 2.0-3.5$  (GeV/c) and  $\sqrt{s} = 44$  (GeV)]. Theoretical studies of large  $p_T$  phenomena, based on elementary exchange dynamics  $^4)$  or on parton ideas  $^5)-7)$ , have suggested a scaling rule, viz.  $E d\sigma/d^3p \propto p_T^{-n} g(p_T/\sqrt{s})$  at  $90^\circ$ , in contrast to the  $s$  independent form  $f(p_T)$  seen at small  $p_T$ . These and other facets of large  $p_T$  phenomena are now under intensive experimental investigation, and it appears useful to develop estimates of results expected on the basis of various theoretical pictures.

In this note we investigate large  $p_T$  behaviour in a simple fragmentation-type model. As sketched in Fig. 1, incident hadrons first scatter at angle  $\Theta$ , thereby becoming excited into states (clusters)  $M_1$  and  $M_2$ , which subsequently disintegrate into observable hadrons. We adopt the usual assumption of fragmentation models that momenta of decay particles transverse to the cluster's line of flight are sharply damped. Particles observed at large  $p_T$  must then originate as longitudinal decays from clusters produced at large angle  $\Theta$ . Using this qualitative picture, with dominance of isospin zero exchange, we readily deduce certain interesting results. These include the asymptotic scaling rule  $g(p_T/\sqrt{s})$  [obtained for essentially the same reason that fragmentation models give Feynman scaling in  $x_L = 2p_L/\sqrt{s}$  at small  $p_T$ ], and the preference for positive charge and for heavier particles at large  $p_T$ . Other results, such as the shape of  $E d\sigma/d^3p$  at fixed  $s$  and associated multiplicities, require an explicit model for the large angle scattering excitation and for the decay of the produced clusters, which we develop below.

### Production model

We use the suggestion of Berman and Jacob  $^8)$  that clusters of mass  $M_1$  and  $M_2$  are produced at large  $t = (\underline{P} - \underline{p}_1)^2$  through a local (vector) current-current interaction (see Fig. 1). Assuming that the structure functions which arise are the same as those in deep inelastic  $e-p$  scattering, they show that  $^*)$

---

$^*)$  This is Eq. (4) of Ref. 8) re-expressed in a different set of variables :  $(M_1^2, P)$  rather than  $(M_1^2, M_2^2, t)$ .

$$\frac{d\sigma_c}{dM_1^2 d^3P} = \frac{C}{\pi s (M_1^2 + P^2)^{1/2}} F_2(\omega_1) F_2(\omega_2) \left( \frac{s^2}{t^2 \omega_1 \omega_2} + \frac{s}{t} + \frac{\omega_1 \omega_2}{2} \right)_{(1)} + (\cos \Theta \rightarrow -\cos \Theta),$$

where C is an over-all normalization constant,  $F_2$  is the usual dimensionless ( $\sqrt{W_2}$ ) structure function, P is the magnitude of the over-all c.m. three-momentum of cluster  $M_1$  and

$$t = M_1^2 + m_p^2 - s^{1/2} (M_1^2 + P^2)^{1/2} + (s - 4m_p^2)^{1/2} P \cos \Theta \quad (2)$$

$$\omega_1 = -t^{-1} \left[ s^{1/2} (M_1^2 + P^2)^{1/2} - 2m_p^2 - (s - 4m_p^2)^{1/2} P \cos \Theta \right] \quad (3)$$

$$\omega_2 = -t^{-1} \left[ s - s^{1/2} (M_1^2 + P^2)^{1/2} - 2m_p^2 - (s - 4m_p^2)^{1/2} P \cos \Theta \right]. \quad (4)$$

Observe that if integrated over all phase space, Eq. (1) leads to a total inelastic cross-section which rises linearly with s. As stressed in Ref. 8), however, the formula is undoubtedly not valid at large  $M_1$ , where natural dynamical cut-offs should remove the linear divergence. This divergence problem is not present in our application, since our interest in large  $p_T$  limits us to a region of small cluster mass [where the factorization assumption explicit in Eq. (1) should be tenable] and thus to a finite portion of  $\sigma_{inel}$ . The fact that large  $M_1$  do not give large  $p_T$  is a major ingredient of our approach and arises through action of the decay distributions described below. We also show below that small  $M_1$  forces  $F_2(\omega_1)$  near to its threshold and provides an inverse power fall-off of  $E d\sigma/d^3p$  in  $p_T$ , consistent with data. For the function  $F_2$  in Eq. (1) we use Miller's fit to the data <sup>9)</sup>

$$F_2(\omega) = 0.56 \left[ (\omega'-1)/\omega' \right]^3 + 2.2 \left[ (\omega'-1)/\omega' \right]^4 - 2.6 \left[ (\omega'-1)/\omega' \right]^5 \quad (5)$$

for  $\omega' \leq 10$ , where  $\omega' = \omega - m_p^2/t$ . For  $\omega' > 10$  we assume  $F_2 = F_2(\omega'=10)$ .

Cluster decay

In explicit applications of fragmentation ideas to analysis of inclusive data <sup>10)</sup>, it is often assumed that produced clusters decay with an average distribution which is isotropic in the cluster rest frame. This approximation, while justifiable at low  $M^2$  and low  $s$ , ceases to be compelling at large  $M^2$  where it may be more reasonable to consider average distributions in the cluster rest frame which are elongated in the direction of the Lorentz boost which takes the cluster to the over-all c.m. frame. In an effort to encompass a fair range of possibilities, we treat decay in two ways : first isotropic, and then very elongated.

In the isotropic case we take the function  $D$  describing the decay (normalized to unity) to be given by

$$\frac{dD}{d^3q} = \frac{1}{a^3 \pi^{3/2}} \exp(-q^2/a^2) \quad (6)$$

where  $q$  is the three momentum of the decay particle (which at present we assume is a pion) in the cluster rest frame and the constant  $a$  sets the scale of  $\langle q^2 \rangle$ . Small  $p_T$  data fix  $a \sim 0.33$  (GeV/c). With isotropic decay, the mean number of pions which decay from the cluster of mass  $M$  is

$$\langle n_\pi \rangle_M = (M - m_p) / (1.5 a^2 + m_\pi^2)^{1/2}. \quad (7)$$

For our situation with (maximum) elongation, we imitate a bremsstrahlung-like result by setting

$$\frac{dD}{d^3q} = \frac{1}{b \pi^{1/2}} \exp(-q_L^2/b^2) \delta^2(q_T) \quad (8)$$

where  $b$  depends on the mass of the cluster, and by taking

$$\langle n_\pi \rangle_M = (M - m_p) / (\frac{1}{2} b^2 + m_\pi^2)^{1/2} = k \ln(M^2/m_p^2); \quad (k \sim 2 \text{ to } 3). \quad (9)$$

Solving this equation for  $b$  we find

$$b^2 = 2 [(M - m_p)^2 - k^2 m_\pi^2 (\ln M^2/m_p^2)^2] / k^2 (\ln M^2/m_p^2)^2. \quad (10)$$

Transforming Eq. (6) to over-all c.m. quantities, we obtain

$$E \frac{dD}{d^3p} = \frac{1}{a^3 \pi^{3/2}} \frac{(\underline{P} \cdot \underline{p})}{M_1} \exp\left[\left(-(\underline{P} \cdot \underline{p})^2/M_1^2 a^2\right) + (m_\pi^2/a^2)\right] \quad (11)$$

where

$$\underline{P} \cdot \underline{p} = (M_1^2 + p^2)^{1/2} (m_\pi^2 + p^2)^{1/2} - P p \cos \psi. \quad (12)$$

Here  $\underline{P}$  and  $\underline{p}$  are the c.m. four-momenta of the cluster and decay pion, respectively,  $P$  and  $p$  are the magnitudes of the corresponding three-momenta and  $\psi$  the angle between them.

Similarly, Eq. (8) becomes

$$E \frac{dD}{d^3p} = \frac{1}{2 b \pi^{3/2}} \frac{(\underline{P} \cdot \underline{p})}{p^2 M_1} \delta(\cos \psi - 1) \exp\left[\left(-(\underline{P} \cdot \underline{p})^2/M_1^2 b^2\right) + (m_\pi^2/b^2)\right]. \quad (13)$$

### Inclusive cross-section

The inclusive cross-section for observation of a hadron decaying from cluster  $M_1$  is

$$E d\sigma/d^3p = \int dM_1^2 d^3P \left(d\sigma_c/dM_1^2 d^3P\right) \langle n \rangle_{M_1} E dD/d^3p \quad (14)$$

Into this expression we substitute Eq. (1) and either Eq. (11) or Eq. (13). Displayed in Fig. 2 is an evaluation of Eq. (14), with the isotropic decay choice (11), at several energies and specialized to a c.m. particle production angle  $\theta = 90^\circ$ . Shown for comparison is a sample of ISR data. Results for other scattering angles will be discussed elsewhere<sup>11)</sup>. The theoretical results provide a  $p_T$  dependence qualitatively similar to that observed at ISR, and a rise with energy of  $E d\sigma/d^3p$  which is also compatible in the range  $3 < p_T < 5$  (GeV/c) with that determined by the Saclay-Strasbourg group.

It is possible to develop from Eq. (14) an approximate equation which shows explicitly the asymptotic scaling nature of our results. For this purpose, we confine ourselves to isotropic decay and for convenience set

$m_\pi = 0$ , neither limitation affecting the scaling behaviour. Inspection of the decay distribution, Eq. (11), shows that the integrand of Eq. (14) is exponentially small unless  $\cos\psi \sim 1$  and  $(M^2/P^2)$  is small. Setting  $\cos\psi = 1$  in the production cross-section, Eq. (1), allows us to perform the angular integrations in Eq. (14) analytically. Introducing the variables  $u = p/P$ ,  $x_1 = (p/\sqrt{s})(1+\cos\theta)$  and  $x_2 = (p/\sqrt{s})(1-\cos\theta)$  and using the restriction to small values of  $(M^2/P^2)$  we obtain the following approximate expression valid at fixed, non-zero  $x_1, x_2$  and sufficiently large  $s$ :

$$E d\sigma/d^3p = p_T^{-8} [g(x_1, x_2) + g(x_2, x_1)] \quad (15)$$

where

$$g(x_1, x_2) = \frac{C (0.56)}{(6\pi^3)^{1/2} a^2} x_1^4 \int_{m_p^2/(1-x_1-x_2)}^{\Delta^2} dM_1^2 (M_1^2)^4 (1 - (m_p/M_1)) \quad (16)$$

$$\int_{x_1+x_2}^{1-(m_p^2/M_1^2)} du u F_2((u-x_1)/x_2) [(u^2+x_1^2)/(u-x_1)] \left\{ \exp[-M_1^2 u^2/(4a^2)] - \exp[-(M_1^2 - m_p^2)/(4M_1^2 a^2)] \right\}$$

For large enough  $s$ ,  $g(x_1, x_2)$  is insensitive to the value  $\Delta^2$  of the cut-off in  $M_1^2$  because of the exponential terms in the integrand. The point that we should like to stress is that the exponential in the decay distribution picks out small values of  $M_1^2$  which, together with large  $p_T$ , forces  $\omega_1'$  near 1, viz.,

$$\omega_1' \sim 1 + (M_1^2 u x_1)/p_T^2 \quad (17)$$

at which point

$$F_2(\omega_1) \sim (\omega_1' - 1)^3 \propto p_T^{-6} \quad (18)$$

Thus there is a close connection between the threshold behaviour of  $F_2$  and the power of  $p_T$  in  $E d\sigma/d^3p$ , here  $p_T^{-8}$ . We obtain the scaling form  $[E d\sigma/d^3p$  proportional to a function of  $(p_T/\sqrt{s})$  at fixed angle or at fixed  $x_L = 2p_L/\sqrt{s}$ ] for essentially the same reason that fragmentation models give Feynman scaling in the longitudinal variable  $x_L$ ; namely, an interval of

masses about a fixed value of  $M_1$  populates a fixed region in  $p/\sqrt{s}$ . Thus the  $p_T^{-n} g(x_1, x_2)$  behaviour, obtained also in more sophisticated approaches, is derived here under dynamical assumptions whose rôle is perhaps more transparent.

In a similar fashion we could obtain a scaling form for the anisotropic decay, which would again have a  $p_T^{-8}$  behaviour, but in this case the distribution is sensitive to the value of  $\Delta^2$ .

### Charge ratios

Estimates of the  $(\pi^+/\pi^-)$  and (total positive/total negative) ratios as a function of  $p_T$  are obtained easily. Since the cluster decay multiplicity is a function of cluster mass  $M_1$ , and a fixed interval in  $M_1$  populates a fixed interval in  $p/\sqrt{s}$ , we expect all charge ratios at  $90^\circ$  to be functions of  $x_T = 2p_T/\sqrt{s}$  and not of  $p_T$  and  $s$  separately. The fact that clusters are positively charged gives an automatic preference for  $(\text{positive/negative}) > 1$ . This effect should increase with  $x_T$  [just as  $(\text{positive/negative})$  ratios increase as a function of  $x_L$  for fixed small  $p_T$ ] since smaller mass clusters [with their smaller decay multiplicities and thus proportionately larger  $\langle n_{+M} \rangle / \langle n_{-M} \rangle$ ] populate larger  $x_T$ .

The total pion multiplicity from isotropic decay is given in Eq. (7). For very large  $M$ ,  $\langle n_{\pi^+} \rangle_M \doteq \langle n_{\pi^-} \rangle_M$ , but this equality is modified substantially at low  $M$  owing to isospin/charge effects. A simple argument suggests

$$\langle n_{\pi^+} \rangle_M = \frac{1}{3} \langle n_\pi \rangle_M + \frac{1}{4} \quad (19)$$

$$\langle n_{\pi^-} \rangle_M = \frac{1}{3} \langle n_\pi \rangle_M - \frac{1}{4} \quad (20)$$

For the total positive multiplicity, we may add  $\frac{1}{2}$  to the right-hand side of Eq. (20), corresponding to the fact that the residual nucleon has roughly equal chance of being either a proton or a neutron :

$$\langle n_{+} \rangle_M = \frac{1}{3} \langle n_\pi \rangle_M + \frac{3}{4} \quad (21)$$

Charge ratios we obtained from these expressions [using Eq. (11)] are shown in Figs. 3a and 3b and are compared with available ISR data.

### Particle ratios

In cluster decay, momentum is shared among decay particles in proportion to their mass ratios. Thus protons take more momentum than pions and, as a result, the  $(p/\pi)$  ratio should increase with  $x_{\perp}$  at  $90^{\circ}$  (just as it increases with  $x_{\perp}$  at fixed small  $p_{\perp}$ ). An estimate of the results expected is obtained by examining data on the  $(p/\pi)$  ratio vs  $x_{\perp}$ . These data <sup>12)</sup> indicate that  $p/\pi^+$  should rise from 1/4 at  $x_{\perp}=0.1$  to 5 at  $x_{\perp}=0.5$ . Data on  $(p/\pi)$  ratios vs  $x_{\perp}$  will provide a good test of the cluster decay picture.

### Associated multiplicities and correlations

An important check on any model for large  $p_{\perp}$  phenomena is its prediction for multiplicity of additional hadrons seen in coincidence with a particle of large  $p_{\perp}$ . Various kinematic regions can be considered.

i) Given a particle observed at  $90^{\circ}$  with large  $p_{\perp}$ , we expect multiplicity observed in a region of solid angle along the incident beam direction to decrease substantially as  $p_{\perp}$  is increased. At least a factor of two decrease should be observed between  $p_{\perp}=0$  and  $p_{\perp}=3$  (GeV/c) in the ISR energy range, inasmuch as the cluster which provides a particle with  $p_{\perp}=3$  (GeV/c) cannot deliver particles along the beam directions. This result is qualitatively consistent with preliminary data <sup>13)</sup>.

ii) Multiplicity in the central region of particles moving in the hemisphere opposite to the observed large  $p_{\perp}$  hadron is expected to increase. Quantitative predictions of our model with isotropic decay are shown in Fig. 3c. Since these opposite hemisphere particles result from decay of clusters with a broad spectrum of masses and momenta, their momentum distribution does not favour large  $p_{\perp}$ .

iii) As stressed above, large  $p_{\perp}$  hadrons originate from low mass <sup>\*)</sup> clusters moving rapidly. This has significant implications for associated multiplicity in the same hemisphere. First, we expect to see a jet of pions with similar values of large  $p_{\perp}$ . Thus, observation of a  $\pi^+$  with large  $p_{\perp}$  implies that a second observed pion (e.g.,  $\pi^0$ ) will have similarly large  $p_{\perp}$ , both  $\pi$ 's having originated from the same cluster. The multiplicity of particles in this highly correlated large  $p_{\perp}$  jet should decrease as  $p_{\perp}$  increases. Second, there may or may not be additional pions with small  $p_{\perp}$ . If present, these arise in our model as spill-over decay

---

\*) Quantitatively, with isotropic decay, we find that cluster masses near  $M = 4.5$  GeV dominate the inclusive  $90^{\circ}$  cross-section at  $s = 2000$  GeV<sup>2</sup> and  $p_{\perp} = 4$  GeV/c.



products of the large mass (opposite hemisphere) second cluster, with observed pions moving against the line of flight of their parent. Inasmuch as we are not confident of our model at large excitation masses, we are unable to estimate this effect. The net associated multiplicity in the same hemisphere as the large  $p_T$  hadron (sum of large  $p_T$  and possible small  $p_T$  components) may then increase as  $p_T$  increases. However, if so, we expect this increase to be provided by  $\pi$ 's with very small  $p_T$ . Our picture is one of a momentum spectrum of same hemisphere associated pions which has a valley between the large  $p_T$  and low  $p_T$  components. It should be very instructive to compare this view of event structure with data. Moreover, the tendency for multiplicity in the central region, in the same jet as the observed particle, to decrease with  $p_T$  seems to be a general feature of models (except perhaps that of Berman, Bjorken and Kogut<sup>5)</sup>) and underlines the great interest in testing this expectation.

Finally, quantum number correlations may be particularly informative. In a multiperipheral approach to large  $p_T$  phenomena<sup>4)</sup>, local conservation of quantum numbers implies that observation of a proton in the central region with large  $p_T$  requires the existence of an antiproton with nearly opposite transverse momentum. No such strong back-to-back correlations are expected in the fragmentation approach. However, for each total jet of particles moving in the transverse direction, we expect to find predominantly net charge  $Q = +1$  and baryon number  $B = +1$ .

Valuable conversations with Dr. Maurice Jacob are acknowledged with gratitude.

R E F E R E N C E S

- 1) CERN-Columbia-Rockefeller-ISR Collaboration;  
B.J. Blumenfeld et al., New York American Physical Society Meeting (1973).
- 2) Saclay-Strasbourg ISR Collaboration;  
M. Banner et al., report submitted to Phys.Letters, March 1973.
- 3) British-Scandinavian ISR Collaboration;  
B. Alper et al., report submitted to Phys.Letters, March 1973.
- 4) D. Amati, L. Caneschi and M. Testa, Phys.Letters 43B, 186 (1973).
- 5) S. Berman, J.D. Bjorken and J. Kogut, Phys.Rev. D4, 3388 (1971).
- 6) R. Blankenbecler, S. Brodsky and J. Gunion, Phys.Rev. D6, 2652 (1972).
- 7) P.V. Landshoff and J.C. Polkinghorne, Cambridge preprints DAMTP 72/43 and 73/10.
- 8) S. Berman and M. Jacob, Phys.Rev.Letters 25, 1683 (1970).
- 9) G. Miller, Ph.D. Thesis, Stanford University, unpublished (1970);  
SLAC Report No. SLAC-129, January 1971.
- 10) See, for example,  
E.L. Berger, M. Jacob and R. Slansky, Phys.Rev. D6, 2580 (1972) and references therein.
- 11) E.L. Berger and D. Branson, CERN report, in preparation.
- 12) M.G. Albrow et al., Phys.Letters 40B, 136 (1972).
- 13) Pisa-Stony Brook ISR Collaboration, as reported by R. Thun in ISR Discussion Meetings (unpublished).

FIGURE CAPTIONS

Figure 1 : Reaction mechanism in which incident particles with momenta  $p_1, p_2$  scatter, giving rise to hadronic clusters with masses  $M_1, M_2$  and over-all c.m. momentum  $P$ ; a disintegration product of cluster  $M_1$  has momentum  $p$ .

Figure 2 : Inclusive cross-section

$$\frac{1}{2} \left[ E \frac{d\sigma}{d^3p} (\pi^+) + E \frac{d\sigma}{d^3p} (\pi^-) \right],$$

obtained from the fragmentation model described in the text, plotted versus  $p_T$  for  $p_L \approx 0$ , and for  $s = 400, 1000, 2000$  and  $3000 \text{ GeV}^2$ . Theoretical results are normalized to the  $\frac{1}{2}(\pi^+ + \pi^-)$  results of Ref. 2) at  $p_T = 4 \text{ GeV}/c$  and  $\sqrt{s} = 44$ . Also shown is a smooth curve interpolated through  $E(d\sigma/d^3p)(\pi^0)$  data of Ref. 1) at  $\sqrt{s} = 53 \text{ GeV}$ . Inset energy dependence of

$$\frac{1}{2} \int_{3.2}^{5.2} \left[ \frac{d\sigma}{d\Omega d^3p} (\pi^+) + \frac{d\sigma}{d\Omega d^3p} (\pi^-) \right] dp_T ;$$

the curve gives results of our calculation; data are from Ref. 2).

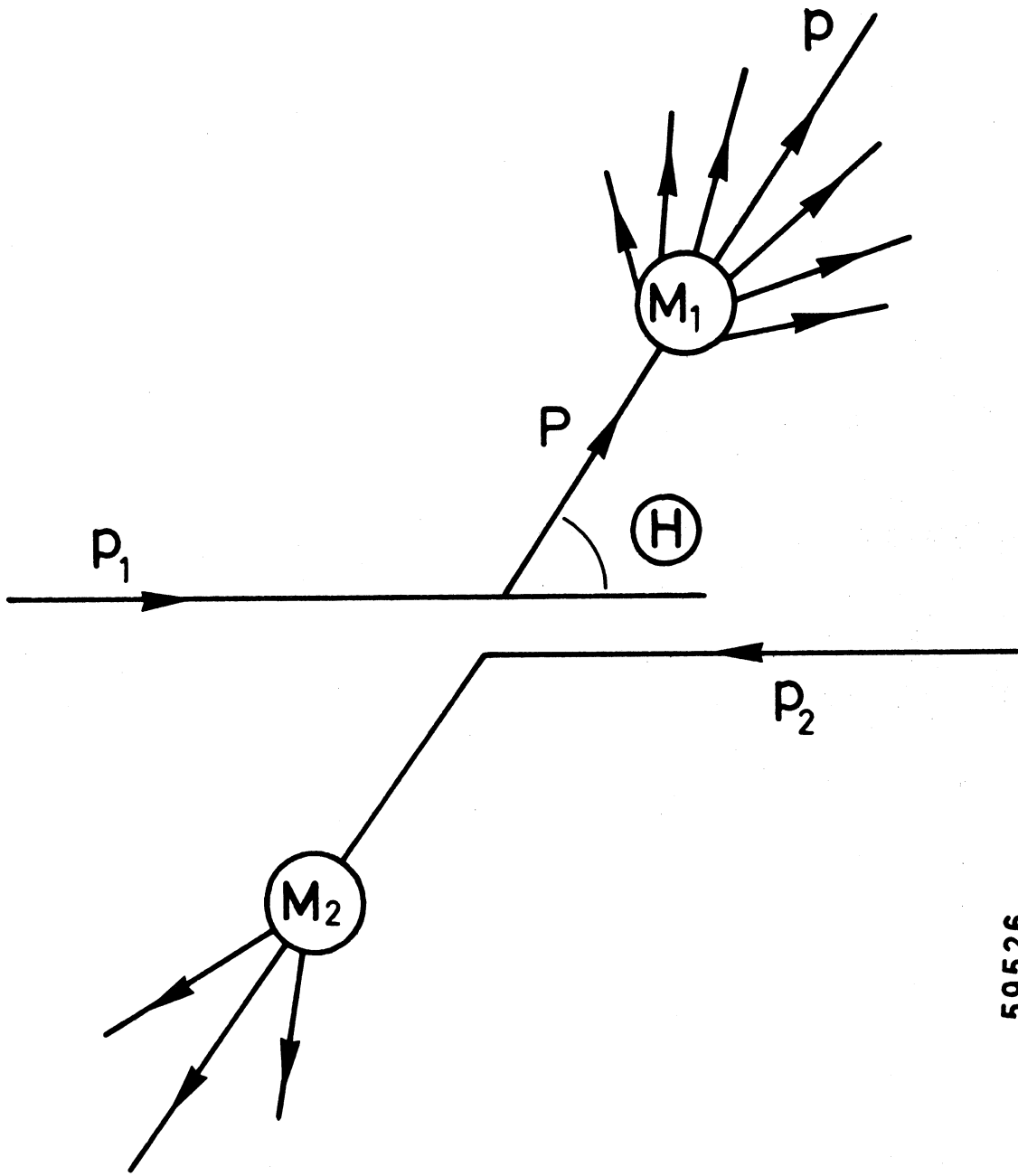
Figure 3a : Predicted values of positive to negative charge ratio

$$(N_+ / N_-) \equiv E d\sigma/d^3p (+) / E d\sigma/d^3p (-)$$

are plotted versus  $x_T = 2p_T/\sqrt{s}$  and compared with data of Ref. 3).

Figure 3b : Our computation of the  $\pi^+$  to  $\pi^-$  production ratio is given as a function of  $x_T$  and compared with data of Ref. 3).

Figure 3c : Given as a function of  $p_T$  are predictions for the increase in average number of charged particles  $\Delta \langle n_{\text{opp}}(p_T) \rangle$  observed in the central region in the hemisphere opposite to a hadron with  $p_L \approx 0$  and given  $p_T$ , and in coincidence with the large  $p_T$  hadron.



59526

Fig. 1

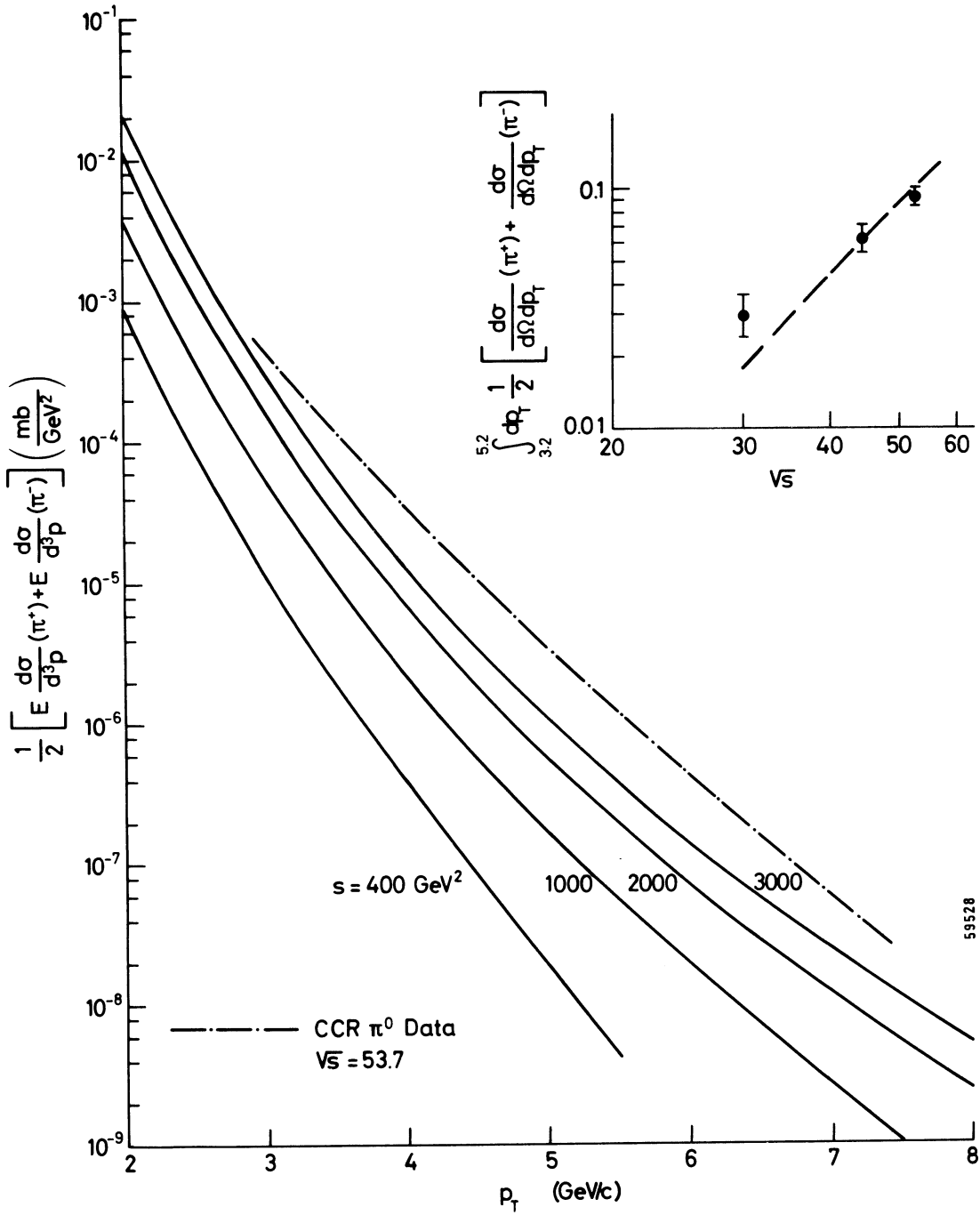


Fig. 2

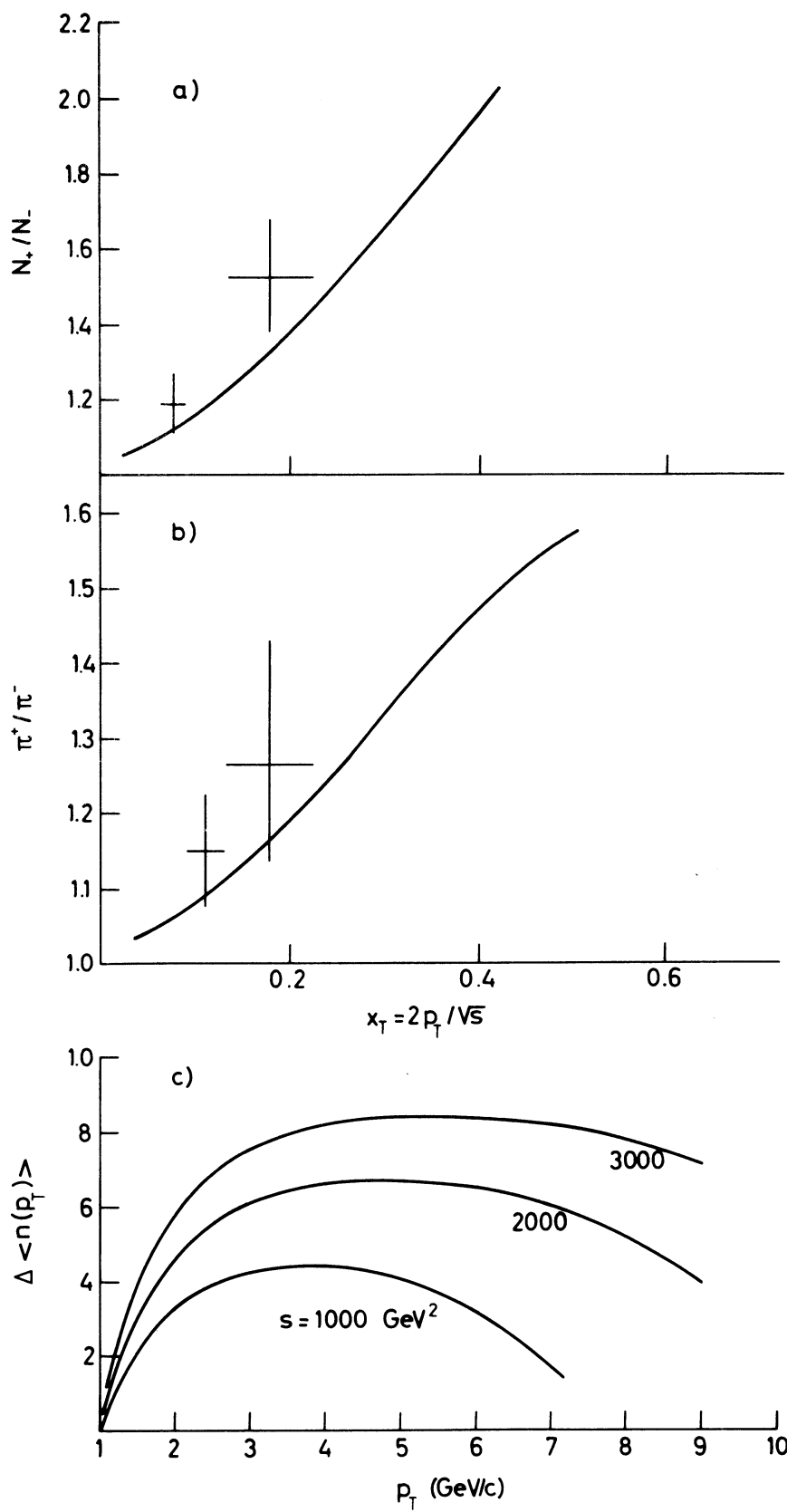


Fig. 3